

This discussion paper is/has been under review for the journal Atmospheric Chemistry and Physics (ACP). Please refer to the corresponding final paper in ACP if available.

Inverse relationship between the degree of oxidation of OOA (oxygenated organic aerosol) and the oxidant OX ($O_3 + NO_2$) due to biogenic emissions

F. Canonaco, J. G. Slowik, U. Baltensperger, and A. S. H. Prévôt

Paul Scherrer Institute, Laboratory of Atmospheric Chemistry, 5232 Villigen PSI, Switzerland

Received: 25 September 2014 – Accepted: 3 October 2014 – Published: 13 November 2014

Correspondence to: F. Canonaco (francesco.canonaco@psi.ch)

Published by Copernicus Publications on behalf of the European Geosciences Union.

Discussion Paper | Discussion Paper

Inverse relationship
between the degree
of oxidation of OOA
and OX due to
biogenic emissions

F. Canonaco et al.

Title Page

Abstract

Introduction

Conclusions

References

Tables

Figures

◀

▶

Back

Close

Full Screen / Esc

Printer-friendly Version

Interactive Discussion

Abstract

Aerosol chemical speciation monitor (ACSM) measurements were performed in Zurich, Switzerland for 13 months (February 2011 through February 2012). Many previous studies using this or related instruments have utilized the fraction of organic mass measured at m/z 44 (f_{44}), which is typically dominated by the CO_2^+ ion and related to oxygenation, as an indicator of atmospheric aging. The current study demonstrates that during summer afternoons, when photochemical processes are most vigorous as indicated by high oxidant OX ($\text{O}_3 + \text{NO}_2$), f_{44} for ambient SOA is not higher but is rather similar or lower than on days with low OX. This is likely due to the formation of semi-volatile oxygenated aerosol produced from biogenic precursor gases, whose emissions increase with ambient temperature.

An additional observation is that in winter often higher f_{44} values in SOA are reached compared to summer. A possible cause could be aqueous processes associated with enhanced relative humidities and cloud cover in winter.

The main changes in f_{44} for the summer case are discussed in the f_{44}/f_{43} space frequently used to interpret ACSM and aerosol mass spectrometer (AMS) data.

In addition, source apportionment analyses conducted on winter and summer data using positive matrix factorization (PMF) yield semi-volatile oxygenated organic aerosol (SV-OOA) factors that retain source-related chemical information. Winter SV-OOA is highly influenced by biomass burning, whereas summer SV-OOA is to a high degree produced from biogenic precursor gases.

1 Introduction

Atmospheric aerosols are at the center of scientific and political discussions due to their highly uncertain direct and indirect climate effects (IPCC, 2007), their adverse impacts on human health (Peng et al., 2005), and their influence on our inhabited (Watson, 2002) and agricultural areas (Matson et al., 2002). Reliable identification and

Title Page	
Abstract	Introduction
Conclusions	References
Tables	Figures
◀	▶
◀	▶
Back	Close
Full Screen / Esc	
Printer-friendly Version	
Interactive Discussion	

quantification of aerosol sources is essential for developing control strategies. The concentrations of particulate matter generally decreased in the last 10–20 years in Europe and Switzerland but legal thresholds are still often exceeded (Barmpadimos et al., 2011, 2012). Atmospheric aerosols are classified based on their formation processes as primary and secondary aerosols, which are directly emitted into the atmosphere and formed from gas-phase to particle conversion, respectively. Recently, scientific focus has shifted towards submicron particulate matter (PM_{1}) (Hallquist et al., 2009), especially the organic fraction, which typically comprises 20–90 % of the total submicron aerosol mass (Jimenez et al., 2009).

Aerodyne aerosol mass spectrometers (AMS), including the aerosol chemical speciation monitor (ACSM), have become important and widely employed instruments for the chemical characterization of submicron organic aerosol (Canagaratna et al., 2007; Ng et al., 2011b). These instruments provide on-line quantitative mass spectra of the non-refractory (inorganic and organic) aerosol composition with high time resolution. Frequently, the organic fraction is further analyzed using the positive matrix factorization algorithm (PMF) proposed by Paatero and Tapper (1994), which represents the organic mass spectral matrix as a set of source/process-related factor mass spectra and time series. Compilation and comparison of northern hemispheric datasets led to the characterization of secondary organic aerosol (SOA)-related factors as semi-volatile and low volatility oxygenated organic aerosol (SV-OOA and LV-OOA) (Jimenez et al., 2009; Ng et al., 2010). The SV-OOA mass spectra have a higher fraction of m/z 43 to organic mass (f_{43}) and a lower fraction of m/z 44 to organic mass (f_{44}) relative to LV-OOA. SV-OOA and LV-OOA factors derived from ambient PMF analyses yield a triangle in the f_{44}/f_{43} space (Ng et al., 2010). SV-OOA usually represents freshly formed OOA, whereas LV-OOA results mostly from photochemical and/or aqueous aging of SV-OOA leading to a net increase of OOA f_{44} with atmospheric age. As shown by Duplissy et al. (2011), organic acids contribute significantly to m/z 44.

Evidence from several smog chamber and ambient studies suggests that the location in the f_{44}/f_{43} space could carry information on the source of SV-OOA. The generation

[Title Page](#)[Abstract](#)[Introduction](#)[Conclusions](#)[References](#)[Tables](#)[Figures](#)[|◀](#)[▶|](#)[Back](#)[Close](#)[Full Screen / Esc](#)[Printer-friendly Version](#)[Interactive Discussion](#)

of SOA from smog chamber indicates that for a given f_{44} , SOA formed from wood burning experiments (Hennigan et al., 2011; Heringa et al., 2011) yields lower f_{43} than from biogenic precursors (Alfarra et al., 2012; Chhabra et al., 2011; Ng et al., 2010; Pfaffenberger et al., 2013). Recently, some ambient studies also showed that the f_{43} and f_{44} points lie in specific regions in the triangular space depending on the season (Crippa et al., 2014; Freney et al., 2011, 2014; Ge et al., 2012). However, the ambient studies showing the raw data points consider the total f_{43} and f_{44} fraction rather than the model-derived OOA. Thus, the position of these points is affected by the contribution of the primary sources, whereas in Ng et al. (2010) the triangular space referred to the modelled OOA factors, i.e. SV-OOA and LV-OOA only.

Photochemical oxidation constitutes a major production pathway for OOA. Tropospheric ozone concentration (O_3) is mainly generated from the oxidation of volatile organic compounds (VOCs) initiated by the OH radical and is thus a useful indicator for photochemical activity. The net oxidation of the simplest VOC, methane, is represented in the presence of NO_x as follows:



The ozone molecules produced by these oxidation reactions participate in a rapid equilibrium between NO and NO_2 , involving the photolysis of NO_2 , summarized by Reaction (R2):



The sum of O_3 and NO_2 concentrations, defined as the oxidant OX (Alghamdi et al., 2014; Clapp and Jenkin, 2001, 2014), is a proxy for the total oxidants formed representing the regional ozone and local NO_x emissions.

Lagrangian studies investigating the evolution of air parcels moving downwind from a city have shown an increase of the LV-OOA to SV-OOA ratio (implying an increase in bulk OOA f_{44}) in parallel to OX formation as a function of the distance from the city center (Jimenez et al., 2009). However, field campaigns and monitoring networks

Title Page

Abstract

Introduction

Conclusions

References

Tables

Figures

|◀

▶|

Back

Close

Full Screen / Esc

Printer-friendly Version

Interactive Discussion



typically rely on stationary measurements, representing Eulerian studies instead, for which the relationship between aging (i.e. OX) and f_{44} is not strictly given.

In this study, ACSM aerosol mass spectra measured in Zurich between February 2011 and February 2012 were analyzed using the PMF algorithm in the multilinear engine (ME-2) implementation. The transformation of the bulk OOA during the aging processes in summer will be related to OX and temperature. Moreover, the OOA composition is characterized in terms of f_{44} and f_{43} , investigating the extent to which precursor sources can be inferred from these values.

2 Materials and methods

10 2.1 Measurements

The instruments and the methods employed for this study were described in detail by Canonaco et al. (2013), and only a brief overview is presented here. An ACSM (Aerodyne Research, Inc., Billerica, MA, USA) was deployed at the Kaserne station, an urban background station in the city center of Zurich (Switzerland), from January 2011 to February 2012. The ACSM is a compact aerosol mass spectrometer designed for long-term measurements of non-refractory particulate matter with vacuum aerodynamic diameters between approximately 60 and 600 nm, typically denoted as NR-PM₁. The instrument is described in detail by Ng et al. (2011b). For a detailed description of operational and analysis principles of the AMS, the reader is referred to Jayne et al. (2000), Jimenez et al. (2003), Allan et al. (2003, 2004), and Canagaratna et al. (2007).

The meteorological data and trace gases were measured with conventional instruments by the Swiss National Air Pollution Monitoring Network, NABEL (Empa, 2011). The time resolution of all these instruments was ten minutes. NO_x was measured by chemiluminescence spectroscopy, whereas UV absorption was employed to estimate the concentration of ozone (Thermo Environmental Instruments (TEI) 49C, Thermo

Title Page

Abstract

Introduction

Conclusions

References

Tables

Figures

|◀

▶|

◀

▶

Back

Close

Full Screen / Esc

Printer-friendly Version

Interactive Discussion

Electron Corp., Waltham, MA). An aethalometer (AE 31, Magee Scientific Inc.) was utilized to retrieve the concentration of equivalent black carbon.

2.2 The multilinear engine (ME-2)

ME-2 (Paatero, 1999) is an engine for solving the positive matrix factorization algorithm (Paatero and Tapper, 1994) where a measured matrix \mathbf{X} is deconvolved into two matrices \mathbf{G} and \mathbf{F} and the remaining residual matrix \mathbf{E} :

$$\mathbf{X} = \mathbf{GF} + \mathbf{E} \quad (1)$$

In the measured matrix \mathbf{X} , the columns j are the m/z 's and each row i represents a single mass spectrum. Note that p is defined as the number of factors of the chosen model solution, i.e. the number of columns of \mathbf{G} and the number of rows of \mathbf{F} . Each column of the matrix \mathbf{G} represents the time series of a factor, whereas each row of \mathbf{F} represents the factor profile (mass spectrum).

In PMF, the entries in \mathbf{G} and \mathbf{F} are fit using a least squares algorithm that minimizes iteratively the quantity Q^m , defined in Eq. (2):

$$Q^m = \sum_{i=1}^m \sum_{j=1}^n \left(\frac{e_{ij}}{\sigma_{ij}} \right)^2 \quad (2)$$

Here e_{ij} are the elements of the residual matrix \mathbf{E} and σ_{ij} are the measurement uncertainties for the input points x_{ij} .

It is well known that PMF solutions suffer from rotational ambiguity (Paatero et al., 2002), i.e. multiple combinations of \mathbf{G} and \mathbf{F} can be found that yield similar Q^m . Thus, the solution space needs to be explored in order to find the most environmentally reasonable and interpretable solution according to the recommendations discussed in Ulbrich et al. (2009), Canonaco et al. (2013) and Crippa et al. (2014).

In this study, rotations are explored using the a value approach, which was first introduced by Lanz et al. (2008) for AMS data, employed for ACSM data in Canonaco

Title Page	
Abstract	Introduction
Conclusions	References
Tables	Figures
◀	▶
◀	▶
Back	Close
Full Screen / Esc	
Printer-friendly Version	
Interactive Discussion	

et al. (2013) and systematically tested on 25 AMS data sets in Crippa et al. (2014). Within this method, the user directs the algorithm towards useful rotations by constraining factor profiles (as done here) and/or factor time series based on a priori information (Paatero and Hopke, 2009).

- 5 Briefly, the a value determines the extent to which a given factor profile ($f_{j,\text{solution}}$) is allowed to vary with respect to its predefined profile value (f_j) during the model iteration:

$$f_{j,\text{solution}} = f_j \pm a \cdot f_j \quad (3)$$

where the index j denotes a measured variable (i.e. m/z) and the a value is its scalar product. As an example, an a value of 0.1 allows for a variability of approximately $\pm 10\%$.

10 For this study we conducted the source apportionment employing the ME-2 solver and constraining the primary sources, i.e. traffic (HOA), cooking (COA) and biomass burning (BBOA) using the a value approach and allowed for two additional free factors representing the secondary components. HOA and COA anchor profiles have been taken from Crippa et al. (2013), where these primary sources have successfully been resolved in an unconstrained PMF run. The BBOA anchor is the averaged BBOA mass spectrum reported in Ng et al. (2011a). The employed a values are 0.1 for HOA and COA and 0.3 for BBOA. This was based on different sensitivity tests performed on the winter and summer data set separately, similar to those presented in Canonaco et al. (2013). The higher a value for BBOA accounts for the fact that the biomass burning sources are more variable, as they depend strongly on the burning material and burning conditions (Hennigan et al., 2011; Heringa et al., 2012; Weimer et al., 2008).

25 2.3 Estimating OOA f_{43} and f_{44}

The approach used in this study for estimating f_{43} and f_{44} for OOA involved the subtraction of the contributions from the primary sources arising at m/z 43 and m/z 44.

[Title Page](#)

[Abstract](#)

[Introduction](#)

[Conclusions](#)

[References](#)

[Tables](#)

[Figures](#)

[|◀](#)

[▶|](#)

[Back](#)

[Close](#)

[Full Screen / Esc](#)

[Printer-friendly Version](#)

[Interactive Discussion](#)



This is slightly different than the method of Ng et al. (2010), where only the modeled f_{43} and f_{44} for SV-OOA and LV-OOA were considered. The two methods produce slightly different results because specific sources/processes are not perfectly represented by individual factors, as evidenced by the residual matrix **E**. In the current method, the variability not captured by the model (i.e. residuals), propagates into the calculated f_{43} and f_{44} . This means that the total OOA variability is more fully captured by the current method, but at the cost of unintentionally including variability due to imperfectly modeled POA.

3 Results and discussion

10 3.1 Source apportionment in winter and summer 2011

Source apportionment was conducted separately for winter (February and March) and summer (June to August) 2011. These two seasons represent extreme cases, whereas spring and fall may be conceptualized as intermediate cases. A complete source apportionment analysis of the ACSM data of 2011/12 is in preparation (Canonaco et al., 15 2014). The summer/winter 2011 results are summarized in the Supplement. Note that the solutions are environmentally reasonable, e.g. the traffic factor correlates with NO_x and EC, the cooking factor peaks at noon in the diurnal cycle, BBOA is higher at night and lower during the day accounting for nocturnal heating in winter and barbecuing and possible local fire events in summer, the daily cycle of SV-OOA is anticorrelated 20 with temperature for the winter and summer data and the daily cycle of LV-OOA shows an increase during the afternoon, most probably representing the conversion between SV-OOA towards LV-OOA.

The OOA f_{44}/f_{43} data together with the ratios of the SV-OOA and LV-OOA in the f_{44}/f_{43} space are summarized for both seasons in Fig. 1. This figure highlights the 25 fact that the majority of the OOA points (gray points), especially those with high masses (data with weak signal to noise is not expected to be explained by the model), are well-

Title Page	
Abstract	Introduction
Conclusions	References
Tables	Figures
◀	▶
◀	▶
Back	Close
Full Screen / Esc	
Printer-friendly Version	
Interactive Discussion	

Title Page

Abstract

Introduction

Conclusions

References

Tables

Figures

◀

▶

◀

▶

Back Close

Full Screen / Esc

Printer-friendly Version

Interactive Discussion

captured by the seasonal PMF run, since they are equally scattered (unimodal residual) around the connection line between SV-OOA and LV-OOA and hardly extend beyond these endpoints. Hence no major systematic over- or underestimations occur. Note that the SV-OOA/LV-OOA connection line is substantially different in winter vs. summer, indicating that a combined winter/summer PMF would fail to capture the seasonal variability in OOA. The winter SV-OOA lies more on the left side of the triangular space, whereas the summer SV-OOA is on the right side of the triangular space. These locations are comparable with the location of SOA from smog chamber studies conducted with biomass burning (Heringa et al., 2011) and biogenic compounds (Pfaffenberger et al., 2013) represented with orange rectangles in Fig. 1a and b, respectively.

3.2 Variations in the f_{44}/f_{43} space for winter 2011

The variation of the winter 2011 OOA points in the f_{44}/f_{43} space shown in Fig. 1a is due to the linear combination between the winter LV-OOA and the biomass burning-related SV-OOA. Adopting the nomenclature convention proposed in Murphy et al. (2014) the winter SV-OOA, called SV-bbSOA (biomass burning SV-OOA), would be due to aging of biomass burning-related VOC's emitted primarily by domestic heating, which peaks at night. Figure S1 supports the interpretation of the winter SV-OOA as originating mainly from biomass burning emissions, due to the presence of m/z 60, the biomass burning tracer (Alfarra et al., 2007) that has been shown to be substantial in SV-bbSOA (Heringa et al., 2011). SV-OOA arising from traffic emissions is likely to be a minor contribution, as the total estimated contribution of the traffic source (combined POA and SOA) for Zurich winter 2011/2012 is on average less than 20 % to the total organics (Zotter et al., 2014). In comparison, the PMF result in this study ascribed on average 12 % to primary traffic contributions, 25 % to SV-OOA and 40 % to LV-OOA. Even if the remaining traffic SOA contribution is completely assumed to be SV-OOA, this would still be a minor part of the total SV-OOA.

SV-bbSOA has a lower f_{44} compared to the SV-OOA in summer (see Sect. 3.3). Nonetheless, the f_{44} of LV-OOA in winter is higher than that of LV-OOA in summer

despite reaching similarly low f_{43} values. A possible explanation could be aqueous-phase production of LV-OOA (either directly or via processing of SV-OOA) in clouds or humidified aerosols, which are believed to increase oxygenation above that predicted by gas-phase reaction/condensation mechanisms (Ervens et al., 2011). However, due to the lack of experimental data and ambient tracers for such mechanisms, this hypothesis remains speculative.

3.3 Variations in the f_{44}/f_{43} space for the summer 2011

3.3.1 General trends

The variation of the summer 2011 OOA data in the f_{44}/f_{43} space shown in Fig. 1 can be described as a linear combination of the summer LV-OOA and SV-OOA (see Sect. 3.2). The relation between temperature and OX for the measured data is shown in Fig. 2a. Note that OX is plotted as a function of the maximal daily temperature ± 2 h to capture the period of highest photochemical activity. This strong relation implies that the photochemical oxidation is highest for days with high temperature. However, the relation between f_{44} and OX is rather flat if not slightly inversely proportional as highlighted in Fig. 2b. On the contrary, f_{43} shows a proportional dependence on the afternoon OX values (Fig. 2c). This is consistent with increased production of SV-OOA relative to LV-OOA, i.e. with increased VOC precursors in the atmosphere. Given the season and elevated temperatures, biogenic emissions are likely a source. Figure 3 illustrates the clustered afternoon data on top of the summer OOA data in the f_{44}/f_{43} space. Only the values in the interval of four hours around the maximal daily temperature (T_{\max}) were considered for the clustering. This figure elucidates the fact that the main horizontal movement of the f_{44}/f_{43} OOA data is driven mainly by temperature and thus by biogenic emissions. Therefore, the modeled SV-OOA is most likely of biogenic nature and can be referred to as SV-bSOA (biogenic SOA) according to Murphy et al. (2014).

Inverse relationship between the degree of oxidation of OOA and OX due to biogenic emissions

F. Canonaco et al.

Title Page

Abstract

Introduction

Conclusions

References

Tables

Figures

◀

▶

◀

▶

Back

Close

Full Screen / Esc

Printer-friendly Version

Interactive Discussion

3.3.2 Day and night variations

Figure 4 shows the OOA data together with two grouped families. The red points are the same as in Fig. 3, i.e. the afternoon values only. The blue points are the clustered points between 0 to 5 a.m. of the following morning. Only early morning points are considered to avoid dilution effects from a rising boundary layer after sunrise. The comparison of the two grouped families (afternoon and early morning) suggests that semi-volatile organics generated during the day condense to the aerosol phase at night, increasing f_{43} and decreasing f_{44} . This effect was already described Lanz et al. (2007) showing that the condensation of freshly oxygenated organic compounds (SV-OOA) was enhanced during the night and the early morning following hot summer days during a three-week campaign with the AMS in Zurich. The fact that the ACSM data from the entire summer season in Zurich in 2011 shows the same temperature-driven partitioning for SV-OOA, reinforces the interpretation of the semi-volatile character of OOA2 from Lanz et al. (2007). As discussed in the previous section, the summer SV-OOA are likely governed by SV-bSOA.

3.3.3 SV-bSOA vs. LV-OOA

SV-bSOA and LV-OOA are plotted against the maximum afternoon temperature as calculated above (red points) and the points between midnight and 5 a.m. of the following morning (blue points) in Fig. 5a and b.

In summer, the SV-bSOA concentration tends to increase as a function of temperature, both during the afternoon and early morning. LV-OOA shows a similar but less pronounced behavior. In Fig. 5c, the ratio (SV-bSOA/total OOA) is plotted against the total OOA mass concentration. For low OOA concentrations, SV-bSOA production is prevailing over LV-OOA. However, the ratio levels off for total OOA mass concentrations above $5 \mu\text{g m}^{-3}$. One possible explanation could involve the departure of the exponential dependency of the biogenic VOC's emission rate from the temperature, which occurs at temperatures between 30 and 35 °C (Smiatek and Steinbrecher, 2006).

Title Page	
Abstract	Introduction
Conclusions	References
Tables	Figures
	
Back	Close
Full Screen / Esc	
Printer-friendly Version	
Interactive Discussion	

Besides the positive trend of SV-OOA with respect to the summer afternoon temperature, the SV-OOA fraction increases as a function of total organic aerosol mass (OA), highlighted in Fig S7. Recently, Pfaffenberger et al. (2013) showed that the partitioning of biogenic semi-volatile organic compounds (SV-OOA) to the aerosol phase is enhanced for increased aerosol mass concentrations. f_{44}/f_{43} plotted as a function of total OA mass ($1.8\text{--}97.2 \mu\text{g m}^{-3}$) for experimental data with similar averaged photochemical age resulted in a slope of approximately -0.017 ± 0.006 per $\mu\text{g m}^{-3}$ (L. Pfaffenberger, personal communication, 2013). In our study the slope of f_{44}/f_{43} vs. the total OA mass excluding data at low OA concentration ($2\text{--}24.7 \mu\text{g m}^{-3}$) was -0.027 ± 0.003 per $\mu\text{g m}^{-3}$. The results suggest a similar behavior, but the retrieved ambient slope is around 1.6 times higher. One reasonable explanation could involve a slightly higher bulk f_{44} value for the ambient data at low concentrations, due to higher photochemical aging. In addition, other reaction pathways, e.g. nitrate oxidation, aqueous phase reactions might also affect the ambient composition and finally, the presence of other ambient VOCs than those tested in the above-mentioned smog chamber study, would also lead to a different ambient slope.

3.3.4 SOA formation in summer

The main ambient emission and photochemical oxidation processes are summarized in Fig. 6. The four sources relevant for this study are represented at the bottom, i.e. biogenic, traffic, cooking and biomass burning. These sources emit VOCs that are transformed to SV-OOA and further to LV-OOA or theoretically directly to LV-OOA (arrows in the figure). Due to a substantial amount of SV-OOA in summer the conversion rate between SV-OOA to LV-OOA is supposed to be smaller compared to the conversion rate of the VOCs to SV-OOA. The amount of OX in the atmosphere is related to the net aging processes and is therefore linked to the conversion from VOC to SV-OOA/LV-OOA and from SV-OOA to LV-OOA. The strong relation between OX and temperature highlighted in Fig. 2a suggests that during the summer afternoon ambient aging is more vigorous. However, Fig. 2b indicates that the bulk OOA f_{44} (LV-OOA) is rather flat with

[Title Page](#)[Abstract](#)[Introduction](#)[Conclusions](#)[References](#)[Tables](#)[Figures](#)[|◀](#)[▶|](#)[◀](#)[▶](#)[Back](#)[Close](#)[Full Screen / Esc](#)[Printer-friendly Version](#)[Interactive Discussion](#)

increasing OX at the expense of the bulk OOA f_{43} (SV-OOA), as also shown in Fig. 3. Higher temperatures will enhance the biogenic emissions relative to the other emission rates. As a consequence the biogenic path will dominate and the resulting SV-OOA will most likely be of biogenic nature, i.e. SV-bSOA, represented as the orange path in Fig. 6.

4 Conclusions

This study shows that the SV-OOA modeled for ambient data by the means of the multilinear engine (ME-2) in winter and in summer retains some chemical information related to its precursor source(s). For a given f_{44} , biomass burning-related SV-OOA (SV-bbSOA) exhibits lower f_{43} relative to biogenic SV-OOA (SV-bSOA), placing these SOAs on the left and right-hand sides of the triangular space identified by Ng et al. (2010), respectively.

Periods of high photochemical activity in summer do not increase the SOA f_{44}/f_{43} ratio because temperature-driven biogenic emissions and subsequent SV-bSOA formation dominate over the conversion rate of SV-OOA to LV-OOA. The f_{44}/f_{43} ratio is consistently lower at night than during the previous day due to the condensation of semi-volatile compounds produced during the day, predominantly from reaction of biogenic VOC's (SV-bSOA).

In summer, the OOA composition depends strongly on temperature and mass concentration for values below $5 \mu\text{g m}^{-3}$. This highlights the importance of biogenic VOC emissions and of the biogenic SOA production.

In addition, there were substantial differences between the winter and summer f_{44}/f_{43} data indicating that a PMF result over the whole data employing two OOA factors only, would fail to fully represent the seasonal variability of OOA.

Title Page

Abstract

Introduction

Conclusions

References

Tables

Figures

◀

▶

◀

▶

Back

Close

Full Screen / Esc

Printer-friendly Version

Interactive Discussion

Acknowledgements. The ACSM measurements were supported by the Swiss Federal Office for the Environment (FOEN). The author would like to thank L. Pfaffenberger and M. Heringa for compiling and providing their smog chamber results in the f44/f43 space, relevant for this publication. Thanks are also due to the Environmental group of the Swiss Federal Laboratories for Materials and Testing (EMPA) for their support and to M. Canonaco and S. Canonaco-Franceschini for a critical reading of this manuscript. J. Slowik acknowledges support from the Swiss National Science Foundation (SNF) through the “Ambizione” program.

References

- Alfarra, M. R., Prevot, A. S. H., Szidat, S., Sandradewi, J., Weimer, S., Lanz, V. A., Schreiber, D., Mohr, M., and Baltensperger, U.: Identification of the mass spectral signature of organic aerosols from wood burning emissions, Environ. Sci. Technol., 41, 5770–5777, 2007.
- Alfarra, M. R., Hamilton, J. F., Wyche, K. P., Good, N., Ward, M. W., Carr, T., Barley, M. H., Monks, P. S., Jenkin, M. E., Lewis, A. C., and McFiggans, G. B.: The effect of photochemical ageing and initial precursor concentration on the composition and hygroscopic properties of β -caryophyllene secondary organic aerosol, Atmos. Chem. Phys., 12, 6417–6436, doi:10.5194/acp-12-6417-2012, 2012.
- Alghamdi, M. A., Khoder, M., Harrison, R. M., Hyvarinen, A. P., Hussein, T., Al-Jeelani, H., Abdelmaksoud, A. S., Goknil, M. H., Shabbaj, I. I., Almehmadi, F. M., Lihavainen, H., Kulmala, M., and Hameri, K.: Temporal variations of O_3 and NO_x in the urban background atmosphere of the coastal city Jeddah, Saudi Arabia, Atmos. Environ., 94, 205–214, 2014.
- Allan, J. D., Delia, A. E., Coe, H., Bower, K. N., Alfarra, M. R., Jimenez, J. L., Middlebrook, A. M., Drewnick, F., Onasch, T. B., Canagaratna, M. R., Jayne, J. T., and Worsnop, D. R.: A generalised method for the extraction of chemically resolved mass spectra from Aerodyne aerosol mass spectrometer data, J. Aerosol Sci., 35, 909–922, 2004.
- Allan, J. D., Jimenez, J. L., Williams, P. I., Alfarra, M. R., Bower, K. N., Jayne, J. T., Coe, H., and Worsnop, D. R.: Quantitative sampling using an Aerodyne aerosol mass spectrometer:

Title Page

Abstract

Introduction

Conclusions

References

Tables

Figures

◀

▶

◀

▶

Back

Close

Full Screen / Esc

Printer-friendly Version

Interactive Discussion



Inverse relationship between the degree of oxidation of OOA and OX due to biogenic emissions

F. Canonaco et al.

1. Techniques of data interpretation and error analysis, *J. Geophys. Res.-Atmos.*, 108, 4090, doi:10.1029/2002JD002358, 2003.
- 5 Barmpadimos, I., Hueglin, C., Keller, J., Henne, S., and Prévôt, A. S. H.: Influence of meteorology on PM₁₀ trends and variability in Switzerland from 1991 to 2008, *Atmos. Chem. Phys.*, 11, 1813–1835, doi:10.5194/acp-11-1813-2011, 2011.
- 10 Barmpadimos, I., Keller, J., Oderbolz, D., Hueglin, C., and Prévôt, A. S. H.: One decade of parallel fine (PM_{2.5}) and coarse (PM₁₀–PM_{2.5}) particulate matter measurements in Europe: trends and variability, *Atmos. Chem. Phys.*, 12, 3189–3203, doi:10.5194/acp-12-3189-2012, 2012.
- 15 Canagaratna, M. R., Jayne, J. T., Jimenez, J. L., Allan, J. D., Alfarra, M. R., Zhang, Q., Onasch, T. B., Drewnick, F., Coe, H., Middlebrook, A., Delia, A., Williams, L. R., Trimborn, A. M., Northway, M. J., DeCarlo, P. F., Kolb, C. E., Davidovits, P., and Worsnop, D. R.: Chemical and microphysical characterization of ambient aerosols with the Aerodyne aerosol mass spectrometer, *Mass Spectrom. Rev.*, 26, 185–222, 2007.
- 20 Canonaco, F., Crippa, M., Slowik, J. G., Baltensperger, U., and Prévôt, A. S. H.: SoFi, an IGOR-based interface for the efficient use of the generalized multilinear engine (ME-2) for the source apportionment: ME-2 application to aerosol mass spectrometer data, *Atmos. Meas. Tech.*, 6, 3649–3661, doi:10.5194/amt-6-3649-2013, 2013.
- 25 Canonaco, F., Dällenbach, K., ElHaddad, I., Crippa, M., Bozzetti, C., Huang, R.-J., Slowik, J., Baltensperger, U., Hüglin, C., Herich, H., and Prevot, A. S. H.: A novel strategy for the source apportionment of long-term ACSM data based on ME-2 with SoFi: automatic rolling SoFi (AuRo-SoFi), in preparation, 2014.
- Chhabra, P. S., Ng, N. L., Canagaratna, M. R., Corrigan, A. L., Russell, L. M., Worsnop, D. R., Flagan, R. C., and Seinfeld, J. H.: Elemental composition and oxidation of chamber organic aerosol, *Atmos. Chem. Phys.*, 11, 8827–8845, doi:10.5194/acp-11-8827-2011, 2011.
- 30 Clapp, L. J. and Jenkin, M. E.: Analysis of the relationship between ambient levels Of O₃, NO₂ and NO as a function of NO chi in the UK, *Atmos. Environ.*, 35, 6391–6405, 2001.
- Crippa, M., DeCarlo, P. F., Slowik, J. G., Mohr, C., Heringa, M. F., Chirico, R., Poulain, L., Freutel, F., Sciare, J., Cozic, J., Di Marco, C. F., Elsasser, M., Nicolas, J. B., Marchand, N., Abidi, E., Wiedensohler, A., Drewnick, F., Schneider, J., Borrmann, S., Nemitz, E., Zimmermann, R., Jaffrezo, J.-L., Prévôt, A. S. H., and Baltensperger, U.: Wintertime aerosol chemical composition and source apportionment of the organic fraction in the metropolitan area of Paris, *Atmos. Chem. Phys.*, 13, 961–981, doi:10.5194/acp-13-961-2013, 2013.

Discussion Paper | Discussion Paper

Discussion Paper | Discussion Paper

Discussion Paper | Discussion Paper

[Title Page](#)

[Abstract](#)

[Introduction](#)

[Conclusions](#)

[References](#)

[Tables](#)

[Figures](#)

[I](#)

[I](#)

[◀](#)

[▶](#)

[Back](#)

[Close](#)

[Full Screen / Esc](#)

[Printer-friendly Version](#)

[Interactive Discussion](#)



Inverse relationship between the degree of oxidation of OOA and OX due to biogenic emissions

F. Canonaco et al.

- Crippa, M., Canonaco, F., Lanz, V. A., Äijälä, M., Allan, J. D., Carbone, S., Capes, G., Ce-
burnis, D., Dall’Osto, M., Day, D. A., DeCarlo, P. F., Ehn, M., Eriksson, A., Freney, E., Hilde-
brandt Ruiz, L., Hillamo, R., Jimenez, J. L., Junninen, H., Kiendler-Scharr, A., Kortelainen, A.-
M., Kulmala, M., Laaksonen, A., Mensah, A. A., Mohr, C., Nemitz, E., O’Dowd, C., Ovad-
nevaite, J., Pandis, S. N., Petäjä, T., Poulain, L., Saarikoski, S., Sellegri, K., Swietlicki, E.,
Tiitta, P., Worsnop, D. R., Baltensperger, U., and Prévôt, A. S. H.: Organic aerosol compo-
nents derived from 25 AMS data sets across Europe using a consistent ME-2 based source
apportionment approach, *Atmos. Chem. Phys.*, 14, 6159–6176, doi:10.5194/acp-14-6159-
2014, 2014.
- Duplissy, J., DeCarlo, P. F., Dommen, J., Alfarra, M. R., Metzger, A., Barmpadimos, I., Pre-
vot, A. S. H., Weingartner, E., Tritscher, T., Gysel, M., Aiken, A. C., Jimenez, J. L., Cana-
garatna, M. R., Worsnop, D. R., Collins, D. R., Tomlinson, J., and Baltensperger, U.: Relating
hygroscopicity and composition of organic aerosol particulate matter, *Atmos. Chem. Phys.*,
11, 1155–1165, doi:10.5194/acp-11-1155-2011, 2011.
- Empa: Technischer Bericht zum Nationalen Beobachtungsnetz für Luftfremdstoffe, (NABEL),
available at: <http://www.empa.ch>, 2011.
- Ervens, B., Turpin, B. J., and Weber, R. J.: Secondary organic aerosol formation in cloud
droplets and aqueous particles (aqSOA): a review of laboratory, field and model studies,
Atmos. Chem. Phys., 11, 11069–11102, doi:10.5194/acp-11-11069-2011, 2011.
- Freney, E. J., Sellegri, K., Canonaco, F., Boulon, J., Hervo, M., Weigel, R., Pichon, J. M.,
Colomb, A., Prévôt, A. S. H., and Laj, P.: Seasonal variations in aerosol particle composi-
tion at the puy-de-Dôme research station in France, *Atmos. Chem. Phys.*, 11, 13047–13059,
doi:10.5194/acp-11-13047-2011, 2011.
- Freney, E. J., Sellegri, K., Canonaco, F., Colomb, A., Borbon, A., Michoud, V., Doussin, J.-F.,
Crumeyrolle, S., Amarouche, N., Pichon, J.-M., Bourianne, T., Gomes, L., Prevot, A. S. H.,
Beekmann, M., and Schwarzenböck, A.: Characterizing the impact of urban emissions on
regional aerosol particles: airborne measurements during the MEGAPOLI experiment, *At-
mos. Chem. Phys.*, 14, 1397–1412, doi:10.5194/acp-14-1397-2014, 2014.
- Ge, X. L., Setyan, A., Sun, Y. L., and Zhang, Q.: Primary and secondary organic aerosols in
Fresno, California during wintertime: results from high resolution aerosol mass spectrometry,
J. Geophys. Res.-Atmos., 117, doi:10.1029/2012JD018026, 2012.
- Hallquist, M., Wenger, J. C., Baltensperger, U., Rudich, Y., Simpson, D., Claeys, M., Dom-
men, J., Donahue, N. M., George, C., Goldstein, A. H., Hamilton, J. F., Herrmann, H., Hoff-

[Title Page](#)

[Abstract](#)

[Introduction](#)

[Conclusions](#)

[References](#)

[Tables](#)

[Figures](#)

[|◀](#)

[▶|](#)

[Back](#)

[Close](#)

[Full Screen / Esc](#)

[Printer-friendly Version](#)

[Interactive Discussion](#)



Inverse relationship between the degree of oxidation of OOA and OX due to biogenic emissions

F. Canonaco et al.

[Title Page](#)

[Abstract](#)

[Introduction](#)

[Conclusions](#)

[References](#)

[Tables](#)

[Figures](#)

[|◀](#)

[▶|](#)

[◀](#)

[▶](#)

[Back](#)

[Close](#)

[Full Screen / Esc](#)

[Printer-friendly Version](#)

[Interactive Discussion](#)

mann, T., Iinuma, Y., Jang, M., Jenkin, M. E., Jimenez, J. L., Kiendler-Scharr, A., Maenhaut, W., McFiggans, G., Mentel, Th. F., Monod, A., Prévôt, A. S. H., Seinfeld, J. H., Suratt, J. D., Szmigielski, R., and Wildt, J.: The formation, properties and impact of secondary organic aerosol: current and emerging issues, *Atmos. Chem. Phys.*, 9, 5155–5236, doi:10.5194/acp-9-5155-2009, 2009.

Hennigan, C. J., Miracolo, M. A., Engelhart, G. J., May, A. A., Presto, A. A., Lee, T., Sullivan, A. P., McMeeking, G. R., Coe, H., Wold, C. E., Hao, W.-M., Gilman, J. B., Kuster, W. C., de Gouw, J., Schichtel, B. A., Collett Jr., J. L., Kreidenweis, S. M., and Robinson, A. L.: Chemical and physical transformations of organic aerosol from the photo-oxidation of open biomass burning emissions in an environmental chamber, *Atmos. Chem. Phys.*, 11, 7669–7686, doi:10.5194/acp-11-7669-2011, 2011.

Heringa, M. F., DeCarlo, P. F., Chirico, R., Tritscher, T., Dommen, J., Weingartner, E., Richter, R., Wehrle, G., Prévôt, A. S. H., and Baltensperger, U.: Investigations of primary and secondary particulate matter of different wood combustion appliances with a high-resolution time-of-flight aerosol mass spectrometer, *Atmos. Chem. Phys.*, 11, 5945–5957, doi:10.5194/acp-11-5945-2011, 2011.

Heringa, M. F., DeCarlo, P. F., Chirico, R., Lauber, A., Doberer, A., Good, J., Nussbaumer, T., Keller, A., Burtscher, H., Richard, A., Miljevic, B., Prevot, A. S. H., and Baltensperger, U.: Time-resolved characterization of primary emissions from residential wood combustion appliances, *Environ. Sci. Technol.*, 46, 11418–11425, 2012.

IPCC: IPCC Fourth Assessment Report: The Physical Science Basis, Working Group I, Final Report, Geneva, Switzerland, 2007.

Jayne, J. T., Leard, D. C., Zhang, X. F., Davidovits, P., Smith, K. A., Kolb, C. E., and Worsnop, D. R.: Development of an aerosol mass spectrometer for size and composition analysis of submicron particles, *Aerosol Sci. Tech.*, 33, 49–70, 2000.

Jenkin, M. E.: Investigation of an oxidant-based methodology for AOT40 exposure assessment in the UK, *Atmos. Environ.*, 94, 332–340, 2014.

Jimenez, J. L., Jayne, J. T., Shi, Q., Kolb, C. E., Worsnop, D. R., Yourshaw, I., Seinfeld, J. H., Flagan, R. C., Zhang, X. F., Smith, K. A., Morris, J. W., and Davidovits, P.: Ambient aerosol sampling using the Aerodyne aerosol mass spectrometer, *J. Geophys. Res.-Atmos.*, 108, 8425, doi:10.1029/2001JD001213, 2003.

Jimenez, J. L., Canagaratna, M. R., Donahue, N. M., Prevot, A. S. H., Zhang, Q., Kroll, J. H., DeCarlo, P. F., Allan, J. D., Coe, H., Ng, N. L., Aiken, A. C., Docherty, K. S., Ulbrich, I. M.,

Inverse relationship between the degree of oxidation of OOA and OX due to biogenic emissions

F. Canonaco et al.

- Grieshop, A. P., Robinson, A. L., Duplissy, J., Smith, J. D., Wilson, K. R., Lanz, V. A., Hueglin, C., Sun, Y. L., Tian, J., Laaksonen, A., Raatikainen, T., Rautiainen, J., Vaattovaara, P., Ehn, M., Kulmala, M., Tomlinson, J. M., Collins, D. R., Cubison, M. J., Dunlea, E. J., Huffman, J. A., Onasch, T. B., Alfarra, M. R., Williams, P. I., Bower, K., Kondo, Y., Schneider, J., Drewnick, F., Borrmann, S., Weimer, S., Demerjian, K., Salcedo, D., Cottrell, L., Griffin, R., Takami, A., Miyoshi, T., Hatakeyama, S., Shimono, A., Sun, J. Y., Zhang, Y. M., Dzepina, K., Kimmel, J. R., Sueper, D., Jayne, J. T., Herndon, S. C., Trimborn, A. M., Williams, L. R., Wood, E. C., Middlebrook, A. M., Kolb, C. E., Baltensperger, U., and Worsnop, D. R.: Evolution of organic aerosols in the atmosphere, *Science*, 326, 1525–1529, 2009.
- Lanz, V. A., Alfarra, M. R., Baltensperger, U., Buchmann, B., Hueglin, C., and Prévôt, A. S. H.: Source apportionment of submicron organic aerosols at an urban site by factor analytical modelling of aerosol mass spectra, *Atmos. Chem. Phys.*, 7, 1503–1522, doi:10.5194/acp-7-1503-2007, 2007.
- Lanz, V. A., Alfarra, M. R., Baltensperger, U., Buchmann, B., Hueglin, C., Szidat, S., Wehrli, M. N., Wacker, L., Weimer, S., Caseiro, A., Puxbaum, H., and Prevot, A. S. H.: Source attribution of submicron organic aerosols during wintertime inversions by advanced factor analysis of aerosol mass spectra, *Environ. Sci. Technol.*, 42, 214–220, 2008.
- Matson, P., Lohse, K. A., and Hall, S. J.: The globalization of nitrogen deposition: consequences for terrestrial ecosystems, *Ambio*, 31, 113–119, 2002.
- Murphy, B. N., Donahue, N. M., Robinson, A. L., and Pandis, S. N.: A naming convention for atmospheric organic aerosol, *Atmos. Chem. Phys.*, 14, 5825–5839, doi:10.5194/acp-14-5825-2014, 2014.
- Ng, N. L., Canagaratna, M. R., Zhang, Q., Jimenez, J. L., Tian, J., Ulbrich, I. M., Kroll, J. H., Docherty, K. S., Chhabra, P. S., Bahreini, R., Murphy, S. M., Seinfeld, J. H., Hildebrandt, L., Donahue, N. M., DeCarlo, P. F., Lanz, V. A., Prévôt, A. S. H., Dinar, E., Rudich, Y., and Worsnop, D. R.: Organic aerosol components observed in Northern Hemispheric datasets from Aerosol Mass Spectrometry, *Atmos. Chem. Phys.*, 10, 4625–4641, doi:10.5194/acp-10-4625-2010, 2010.
- Ng, N. L., Canagaratna, M. R., Jimenez, J. L., Zhang, Q., Ulbrich, I. M., and Worsnop, D. R.: Real-time methods for estimating organic component mass concentrations from aerosol mass spectrometer data, *Environ. Sci. Technol.*, 45, 910–916, 2011a.

Title Page	Abstract	Introduction
Conclusions	References	
Tables	Figures	
◀	▶	
Back	Close	
Full Screen / Esc		
Printer-friendly Version		
Interactive Discussion		

- Ng, N. L., Herndon, S. C., Trimborn, A., Canagaratna, M. R., Croteau, P. L., Onasch, T. B., Sueper, D., Worsnop, D. R., Zhang, Q., Sun, Y. L., and Jayne, J. T.: An aerosol chemical speciation monitor (ACSM) for routine monitoring of the composition and mass concentrations of ambient aerosol, *Aerosol Sci. Tech.*, 45, 770–784, 2011b.
- 5 Paatero, P.: The multilinear engine - A table-driven, least squares program for solving multilinear problems, including the n-way parallel factor analysis model, *J. Comput. Graph. Stat.*, 8, 854–888, 1999.
- Paatero, P. and Hopke, P. K.: Rotational tools for factor analytic models, *J. Chemometrics*, 23, 91–100, 2009.
- 10 Paatero, P. and Tapper, U.: Positive matrix factorization – a nonnegative factor model with optimal utilization of error-estimates of data values, *Environmetrics*, 5, 111–126, 1994.
- Paatero, P., Hopke, P. K., Song, X. H., and Ramadan, Z.: Understanding and controlling rotations in factor analytic models, *Chemometr. Intell. Lab.*, 60, 253–264, 2002.
- 15 Peng, R. D., Dominici, F., Pastor-Barriuso, R., Zeger, S. L., and Samet, J. M.: Seasonal analyses of air pollution and mortality in 100 US cities, *Am. J. Epidemiol.*, 161, 585–594, 2005.
- Pfaffenberger, L., Barmet, P., Slowik, J. G., Praplan, A. P., Dommen, J., Prévôt, A. S. H., and Baltensperger, U.: The link between organic aerosol mass loading and degree of oxygenation: an α -pinene photooxidation study, *Atmos. Chem. Phys.*, 13, 6493–6506, doi:10.5194/acp-13-6493-2013, 2013.
- 20 Smiatek, G. and Steinbrecher, R.: Temporal and spatial variation of forest VOC emissions in Germany in the decade 1994–2003, *Atmos. Environ.*, 40, S166–S177, 2006.
- Ulbrich, I. M., Canagaratna, M. R., Zhang, Q., Worsnop, D. R., and Jimenez, J. L.: Interpretation of organic components from Positive Matrix Factorization of aerosol mass spectrometric data, *Atmos. Chem. Phys.*, 9, 2891–2918, doi:10.5194/acp-9-2891-2009, 2009.
- 25 Watson, J. G.: Visibility: science and regulation, *J. Air Waste Manage.*, 52, 628–713, 2002.
- Weimer, S., Alfarra, M. R., Schreiber, D., Mohr, M., Prevot, A. S. H., and Baltensperger, U.: Organic aerosol mass spectral signatures from wood-burning emissions: influence of burning conditions and wood type, *J. Geophys. Res.-Atmos.*, 113, doi:10.1029/2007JD009309, 2008.
- 30 Zotter, P., Ciobanu, V. G., Zhang, Y. L., El-Haddad, I., Macchia, M., Daellenbach, K. R., Salazar, G. A., Huang, R.-J., Wacker, L., Hueglin, C., Piazzalunga, A., Fermo, P., Schwikowski, M., Baltensperger, U., Szidat, S., and Prévôt, A. S. H.: Radiocarbon analysis of elemental and organic carbon in Switzerland during winter-smog episodes from 2008

[Title Page](#)[Abstract](#)[Introduction](#)[Conclusions](#)[References](#)[Tables](#)[Figures](#)[|◀](#)[▶|](#)[◀](#)[▶](#)[Back](#)[Close](#)[Full Screen / Esc](#)[Printer-friendly Version](#)[Interactive Discussion](#)

**Inverse relationship
between the degree
of oxidation of OOA
and OX due to
biogenic emissions**

F. Canonaco et al.

[Title Page](#)

[Abstract](#)

[Introduction](#)

[Conclusions](#)

[References](#)

[Tables](#)

[Figures](#)

◀

▶

[Back](#)

[Close](#)

[Full Screen / Esc](#)

[Printer-friendly Version](#)

[Interactive Discussion](#)

Inverse relationship between the degree of oxidation of OOA and OX due to bioactive emissions

F. Canonaco et al.

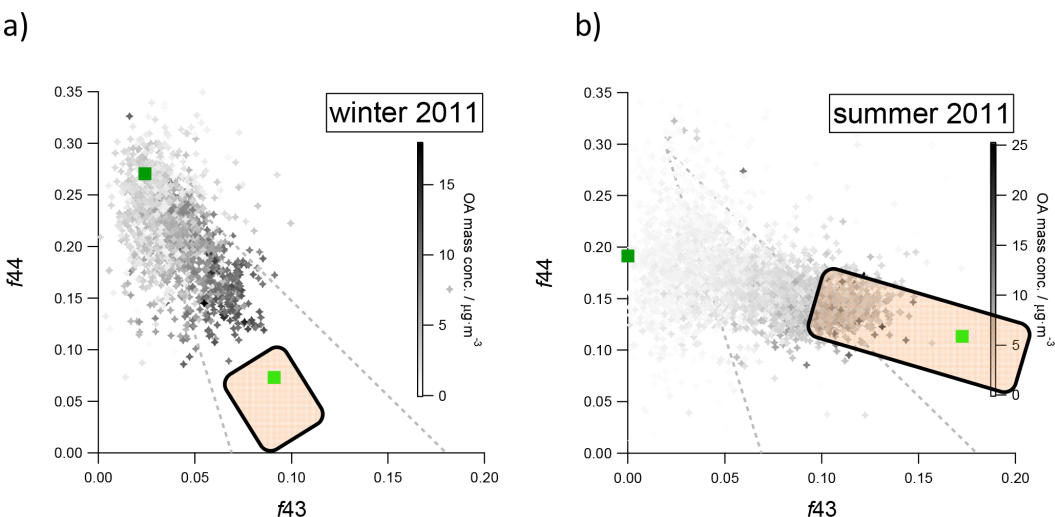


Figure 1. Gray points represent the estimated SOA f_{44} and f_{43} for winter 2011 (**a**) and summer 2011 (**b**). The data is color-coded based on the total OA mass concentration. The green points are the f_{44} and f_{43} ratios of SV-OOA (light green) and LV-OOA (dark green). Orange rectangles represent the composition of SOA from smog chamber experiments using biomass burning (**a**) and α -pinene (**b**) precursors (Heringa et al., 2011; Pfaffenberger et al., 2013).

28099

Title Page	
Abstract	Introduction
conclusions	References
Tables	Figures
◀	▶
◀	▶
Back	Close
Full Screen / Esc	



Inverse relationship between the degree of oxidation of OOA and OX due to bioactive emissions

F. Canonaco et al.

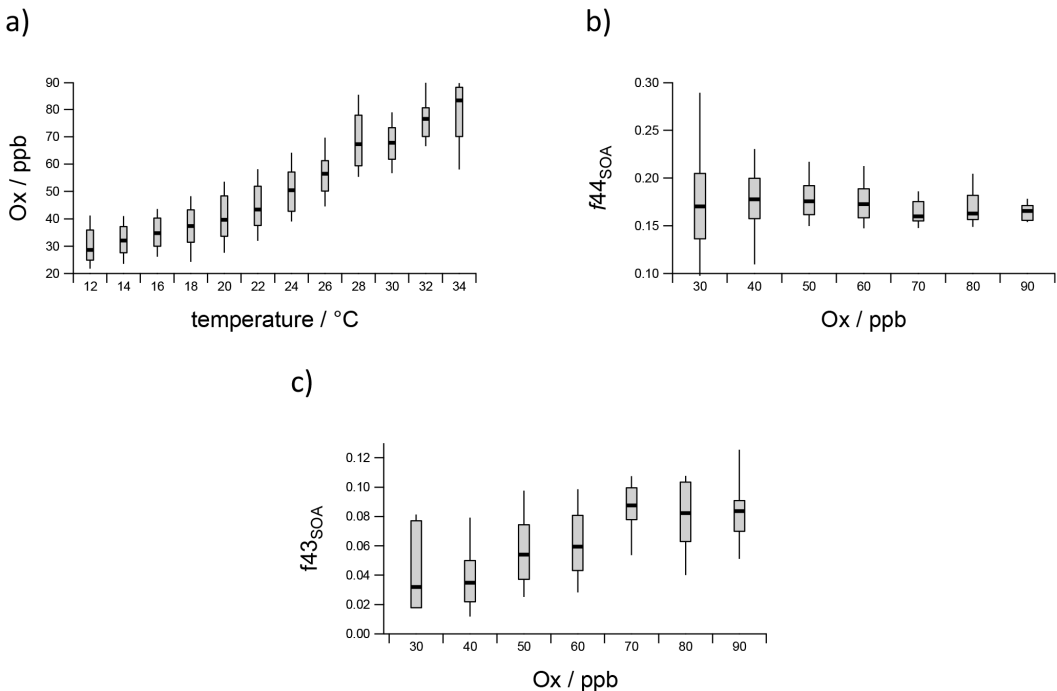


Figure 2. The three box plots represent: **(a)** OX as a function of afternoon temperature ($T_{\max} \pm 2$ h), **(b)** SOA f_{44} as a function of afternoon OX and **(c)** SOA f_{43} as a function of afternoon OX. The horizontal lines denote the median, the boxes span the quartiles and the whiskers represent the 10th and 90th percentiles, respectively.

28100

**Inverse relationship
between the degree
of oxidation of OOA
and OX due to
biogenic emissions**

F. Canonaco et al.

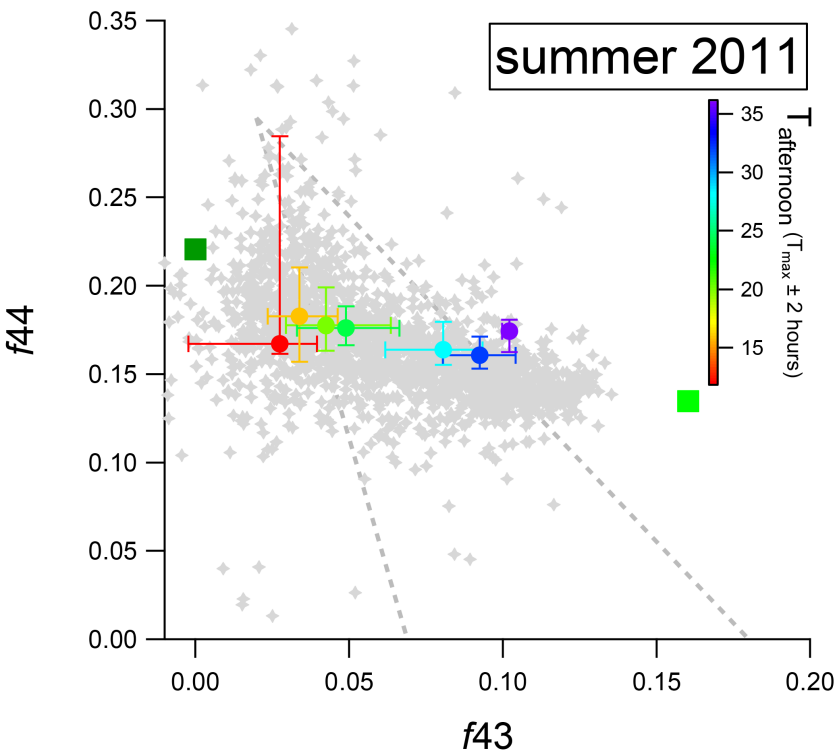


Figure 3. SOA f_{44} vs. f_{43} for all data points in summer 2011 (gray dots) and LV-OOA/SV-OOA factors (green squares). Color-coded circles denote averages at the daily maximum temperature (T_{\max}) ± 2 h.

**Inverse relationship
between the degree
of oxidation of OOA
and OX due to
biogenic emissions**

F. Canonaco et al.

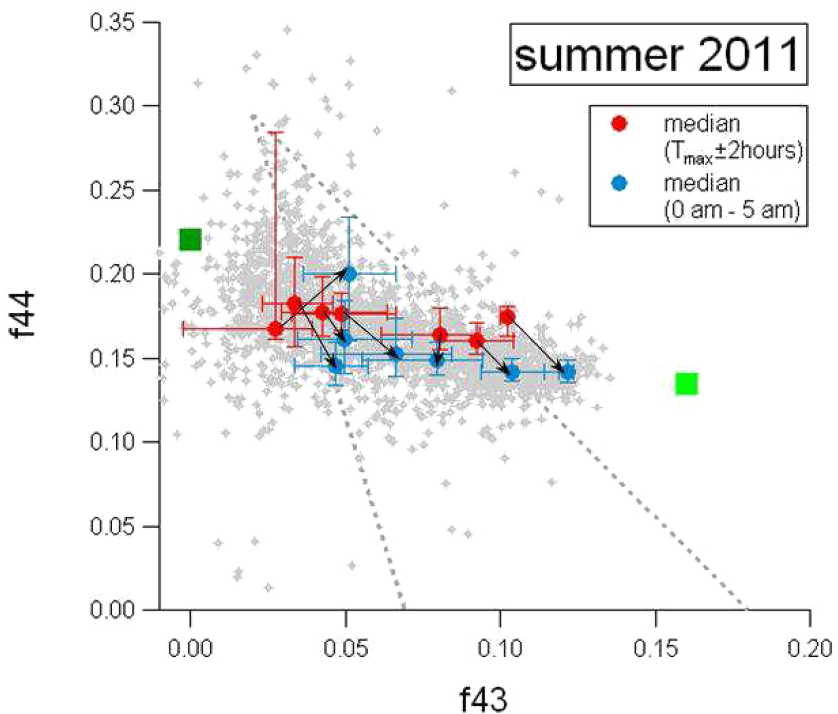


Figure 4. SOA f_{44} vs. f_{43} for all data points in summer 2011 (gray dots) and LV-OOA/SV-OOA factors (green squares). Red circles denote daily $T_{\max} \pm 2\text{ h}$, while blue circles denote the average over the following midnight to 5 a.m. period. Black arrows connect corresponding day and night averages.

Inverse relationship between the degree of oxidation of OOA and OX due to biogenic emissions

F. Canonaco et al.

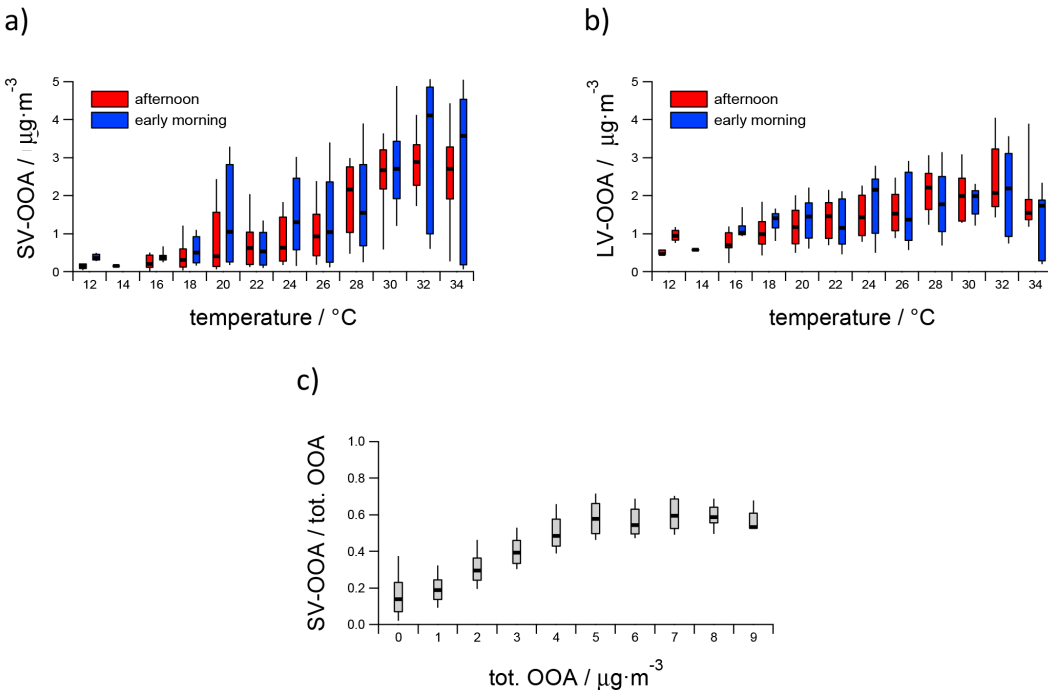


Figure 5. Box plots describing OOA composition, where horizontal lines indicate median values, boxes denote quartiles, and whiskers represent 10th and 90th percentiles. The afternoon and early morning points are estimated as $T_{\max} \pm 2$ h and midnight to 5 a.m., respectively. Quantities plotted are SV-OOA vs. temperature (**a**), LV-OOA vs. temperature (**b**), and SV-OOA fraction vs. total OOA mass (**c**).

Title Page	Abstract	Introduction
Conclusions	References	
Tables	Figures	
		
		Close
Full Screen / Esc		
Printer-friendly Version		
Interactive Discussion		

Inverse relationship between the degree of oxidation of OOA and OX due to bioactive emissions

F. Canonaco et al.

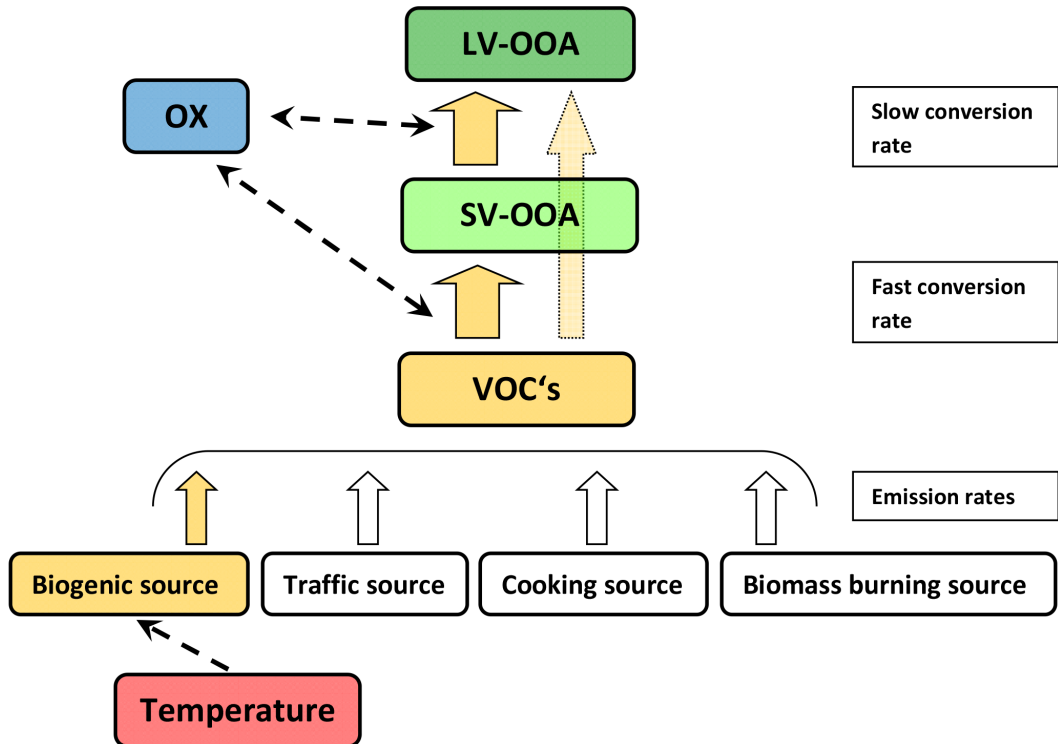


Figure 6. The simplified scheme represents the emissions and aging processes occurring in ambient during summer afternoons. The big arrows stand for the emission/conversion rates and the dashed arrows show qualitative dependencies, with the arrow pointing towards the dependent quantity. Higher temperatures in summer primarily enhance the biogenic path (highlighted in orange).